# Quantum Monte Carlo algorithm for out-of-equilibrium Green's functions at long times

Corentin Bertrand[1], Olivier Parcollet,[2,3] Antoine Maillard,[4] and Xavier Waintal[1]

[1]*Université Grenoble Alpes, CEA, INAC-PHELIQS, GT F-38000 Grenoble, France*
[2]*Center for Computational Quantum Physics, Flatiron Institute, 162 5th Avenue, New York 10010, USA*
[3]*Institut de Physique Théorique (IPhT), CEA, CNRS, UMR 3681, 91191 Gif-sur-Yvette, France*
[4]*Laboratoire de Physique de l'Ecole Normale Supérieure, UMR 8550, 24 Rue Lhomond, 75005 Paris, France*

We present a quantum Monte Carlo algorithm for computing the perturbative expansion in power of the coupling constant $U$ of the out-of-equilibrium Green's functions of interacting Hamiltonians of fermions. The algorithm extends the one presented in Profumo *et al.* [Phys. Rev. B **91**, 245154 (2015)], and inherits its main property: it can reach the infinite time (steady state) limit since the computational cost to compute order $U^n$ is uniform versus time; the computing time increases as $2^n$. The algorithm is based on the Schwinger-Keldysh formalism and can be used for both equilibrium and out-of-equilibrium calculations. It is stable at both small and long real times including in the stationary regime, because of its automatic cancellation of the disconnected Feynman diagrams. We apply this technique to the Anderson quantum impurity model in the quantum dot geometry to obtain the Green's function and self-energy expansion up to order $U^{10}$ at very low temperature. We benchmark our results at weak and intermediate coupling with high precision numerical renormalization-group computations as well as analytical results.

## I. INTRODUCTION

The study of the out-of-equilibrium regime of strongly correlated many-body quantum problems is a subject of growing interest in theoretical condensed-matter physics, in particular due to a rapid progress in experiments with, e.g., the ability to control light-matter interaction on the ultrafast time scale [1], light-induced superconductivity [2–6], or metal-insulator transition driven by electric field [7]. The development of high precision and controlled computational methods for nonequilibrium models in strongly correlated regimes is therefore very important. Even within an approximated framework such as dynamical mean-field theory [8–10] (DMFT), which reduces the bulk lattice problem to the solution of a self-consistent quantum impurity model, efficient numerically exact real time out-of-equilibrium quantum impurity solver algorithms are still lacking.

The long-time steady state of nonequilibrium strongly interacting quantum systems is especially difficult to access within high-precision numerical methods. Until recently, most approaches were severely limited in reaching long times, e.g., the density matrix renormalization group (DMRG) [11–13] faces entanglement growth at long times. Early attempts of real time quantum Monte Carlo [14–18] also experienced an exponential sign problem at long times and large interaction. Within Monte Carlo methods, two main routes are currently explored to resolve this issue: the inchworm algorithm [19–23] and the so-called "diagrammatic" quantum Monte Carlo [24] (QMC). Diagrammatic QMC [25–40] computes the perturbative expansion of physical quantities in power of the interaction $U$, using an importance sampling Monte Carlo. In Ref. [24], some of us have shown that, when properly generalized to the Schwinger-Keldysh formalism,

this approach yields the perturbative expansion in the steady state, i.e., at infinite time. We showed that, by regrouping the Feynman diagrams into determinants and summing explicitly on the Keldysh indices of the times of the vertices of the expansion, we eliminate the vacuum diagrams and obtain a clusterization property allowing us to take the long-time limit. The sum over the Keldysh indices implies a minimal cost of $O(2^n)$ to compute the order $n$, but *uniformly in time*, at any temperature. We refer to this class of algorithms as "diagrammatic" for historical reasons, as their first versions (in imaginary time) were using an explicit Markov chain in the space of Feynman diagrams. However, modern versions of the algorithms regroup diagrams with only an exponential number of determinants (instead of sampling the $n!$ diagrams), eliminating the vacuum diagrams, both in real time [24] and in imaginary time [41,42], which leads to much higher performance.

In this paper, we generalize the algorithm presented in Ref. [24] to the calculations of Green's functions. Indeed, in its initial formulation it only permits the calculation of physical observables at equal time such as the density or current, and the full Green's function requires the computation of each time one by one, which is not technically viable. Here, we show how to use a kernel technique in order to obtain efficiently the perturbative expansion of the Green's function and the self-energy, as a function of time or frequency. Computing the Green's function is an important extension of the technique. First, it is the first step towards building a DMFT real time nonequilibrium impurity solver. Second, even in the simple context of a quantum dot, each computation provides much more information than the original algorithm (from which only a single number, e.g., the current, could be computed).

The central issue of the "diagrammatic" QMC family is to properly sum the perturbative expansion away from the weak-coupling regime, especially given the fact that one has access to a limited number of orders (about ten in the present case) due to the exponential cost with the order $n$. Some of us will address this issue in a separate paper [43], using the building blocks introduced here. In this paper, we present the formalism and first benchmark our approach in the weak-coupling regime.

This paper is organized as follows: In Sec. II, we introduce the necessary formalism and derive the basic equations that will be used to formulate the method. Section III discusses our sampling strategy for the QMC algorithm, as well as relations with previous work. Section IV shows our numerical data and the detailed comparison with our benchmarks in the weak-coupling regime.

## II. WICK DETERMINANT FORMALISM

This section is devoted to the derivation of the main formula needed to set up the QMC technique. We introduce a systematic formalism that uses what we call "Wick determinants". Although the formalism is nothing but the usual diagrammatic expansion (in Keldysh space), its Wick determinant formulation provides a route for deriving standard results (such as equation of motions) in a self-contained manner that does not require us to introduce Feynman diagrams. We find this approach useful for discussing numerical algorithms.

### A. Notations and main expansion formula

We consider a generic class of system given by a time-dependent Hamiltonian of the form

$$\hat{\mathbf{H}}(t) = \hat{\mathbf{H}}_0(t) + U\,\hat{\mathbf{H}}_{\text{int}}(t), \tag{1}$$

$$\hat{\mathbf{H}}_0(t) = \sum_{xy} \mathbf{H}^0_{xy}(t)\hat{\mathbf{c}}^\dagger_x \hat{\mathbf{c}}_y, \tag{2}$$

$$\hat{\mathbf{H}}_{\text{int}}(t) = \sum_{xy} V_{xy}(t)(\hat{\mathbf{c}}^\dagger_x \hat{\mathbf{c}}_x - \alpha_x)(\hat{\mathbf{c}}^\dagger_y \hat{\mathbf{c}}_y - \alpha_y), \tag{3}$$

where $\hat{\mathbf{H}}_0(t)$ is a quadratic unperturbed Hamiltonian. The operators $\hat{\mathbf{c}}^\dagger_x$ ($\hat{\mathbf{c}}_x$) are the usual creation (destruction) operators on site $x$. $x$ and $y$ index all discrete degrees of freedom such as sites, orbitals, spin, and/or electron-hole (Nambu) degrees of freedom and will simply be called orbital indices. $\hat{\mathbf{H}}_{\text{int}}(t)$ is the, possibly, time-dependent, electron-electron interaction perturbation which is assumed to be switched on at $t = 0$. Without loss of generality we assume $V_{xy} = V_{yx}$. We emphasize that the method described in this paper is not restricted to this form of interaction (as shown in Ref. [24]) and can be generalized straightforwardly to arbitrary interactions. However, to improve readability, we will restrict hereafter our presentation to the case of density-density interactions. We also add the quadratic shift $\alpha$, which has been introduced in previous works [24,44,45]. In particular, we have shown in Ref. [24] that, in the context of real time QMC, it can strongly affect the radius of convergence of the perturbative series. The noninteracting Hamiltonian is assumed to be already solved, i.e., one has calculated all the one-particle noninteracting

Green's functions. Such calculations can be done even out of equilibrium using, e.g., the formalism discussed in Ref. [46].

Our starting point is a formula for the systematic expansion of interacting Green's function in powers of the parameter $U$. We use the Schwinger-Keldysh formalism to produce this expansion. The Green's functions acquire additional Keldysh indices $a, a' \in \{0, 1\}$ which provides the Green's function with a $2 \times 2$ structure,

$$G^{aa'}_{xx'}(t, t') = \begin{pmatrix} G^T_{xx'}(t, t') & G^<_{xx'}(t, t') \\ G^>_{xx'}(t, t') & G^{\bar{T}}_{xx'}(t, t') \end{pmatrix}, \tag{4}$$

where $G^T_{xx'}(t, t')$, $G^<_{xx'}(t, t')$, $G^>_{xx'}(t, t')$, and $G^{\bar{T}}_{xx'}(t, t')$ are respectively the standard time ordered, lesser, greater, and antitime ordered Green's functions. We use a similar definition for the (known) noninteracting Green's function $g^{aa'}_{xx'}(t, t')$. We introduce the Keldysh points $X$ that gather an orbital index $x$, a time $t$, and a Keldysh index $a$ to form the tuple $X \equiv (x, t, a)$. Using Keldysh points, we can rewrite the above definitions using the standard conventions of Keldysh formalism,

$$G^{aa'}_{xx'}(t, t') \equiv -i\langle T_c \hat{\mathbf{c}}(x, t, a)\hat{\mathbf{c}}^\dagger(x', t', a')\rangle, \tag{5}$$

where the creation $[\hat{\mathbf{c}}^\dagger(X')]$ and annihilation operators $[\hat{\mathbf{c}}(X)$ or $\hat{\mathbf{c}}(x, t, a)]$, here in Heisenberg representation, are ordered using the contour time-ordering operator $T_c$. $T_c$ orders first by Keldysh index ($a$) before ordering by increasing time within the forward branch ($a = 0$), and by decreasing time within the backward branch ($a = 1$) eventually multiplying the result by the usual fermionic ($-1$) factor whenever an odd number of permutations have been performed. In several places, we will use the alternative notation for the Green's function,

$$G(X, X') \equiv G[(x, t, a), (x', t', a')] \equiv G^{aa'}_{xx'}(t, t'), \tag{6}$$

and we will also note the $\delta$ function on the Keldysh contour as

$$\delta_c[(x, t, a), (x', t', a')] \equiv \delta(t - t')\delta_{aa'}\delta_{xx'}. \tag{7}$$

Using the above notations (with $\hbar = 1$), one can derive the usual expansion in power of $U$ using Wick's theorem. We first assume $\alpha_x = 0$ at all orbital indices $x$. We will explain at the end of this paragraph how to extend this formula to the general case $\alpha_x \neq 0$. We obtain [24]

$$G^{aa'}_{xx'}(t, t')$$

$$= \sum_{n \geqslant 0} \frac{i^n U^n}{n!} \int \prod_{k=1}^{n} du_k \sum_{\{x_k, y_k\}} \sum_{\{a_k\}}$$

$$\times \left(\prod_{k=1}^{n}(-1)^{a_k} V_{x_k y_k}(u_k)\right) \left[\!\!\left[\begin{matrix} (x, t, a), U_1, \ldots, U_{2n} \\ (x', t', a'), U_1, \ldots, U_{2n} \end{matrix}\right]\!\!\right], \tag{8}$$

which forms the starting point of this work. Here, we have noted for $1 \leqslant k \leqslant n$

$$U_{2k-1} = (x_k, u_k, a_k), \tag{9a}$$

$$U_{2k} = (y_k, u_k, a_k) \tag{9b}$$

and introduced the *Wick matrix*:

$$\left[\!\!\left[\begin{matrix} A_1, \ldots, A_m \\ B_1, \ldots, B_m \end{matrix}\right]\!\!\right]_{ij} \equiv \begin{pmatrix} g(A_1, B_1) & \ldots & g(A_1, B_m) \\ \vdots & \ddots & \vdots \\ g(A_m, B_1) & \ldots & g(A_m, B_m) \end{pmatrix}_{ij}, \tag{10}$$

where $A_i$ and $B_j$ are two sets of $m$ points on the Keldysh contour. We refer to the determinant of the Wick matrix as the *Wick determinant*. For notation simplicity, the determinant is assumed in the absence of indices,

$$\begin{bmatrix} A_1, \ldots, A_m \\ B_1, \ldots, B_m \end{bmatrix} \equiv \det \begin{bmatrix} A_1, \ldots, A_m \\ B_1, \ldots, B_m \end{bmatrix}_{ij}. \qquad (11)$$

In Eq. (8), we start at $t < 0$ with a noninteracting state and switch on the interaction for $t \geqslant 0$. Hence the time integrals in Eq. (8) run over the segment $[0, t_M]$, where $t_M = \max(t, t')$. The lower boundary simply arises from $V_{xy}(u < 0) = 0$. The upper boundary can be extended to any value larger than $t_M$ without changing the integral's value (standard property of the Keldysh formalism). For the practical applications shown in Sec. III, we will use a fixed large value of $t_M$. We emphasize that the complexity of the algorithm does *not* grow with $t_M$. Equation (8) is formally very appealing: it reduces the problem of calculating the contributions of the expansion to a combination of linear algebra and quadrature.

The definition Eq. (10) contains an ambiguity that needs to be clarified: the ordering at equal times of terms like $g(U_{2k}, U_{2k})$ is ill defined. For these terms, one must keep the same ordering of the creation and destruction operators as in the original definition of the interacting Hamiltonian Eq. (1), i.e.,

$$g(U_{2k}, U_{2k}) = g^<_{y_k y_k}(u_k, u_k), \qquad (12a)$$

$$g(U_{2k-1}, U_{2k-1}) = g^<_{x_k x_k}(u_k, u_k), \qquad (12b)$$

$$g(U_{2k-1}, U_{2k}) = g^>_{x_k y_k}(u_k, u_k), \qquad (12c)$$

$$g(U_{2k}, U_{2k-1}) = g^<_{y_k x_k}(u_k, u_k). \qquad (12d)$$

To proceed to the general case $\alpha_x \neq 0$, one only needs to shift the diagonal terms of the Wick matrix using the following replacement rules, as shown in Ref. [24], Appendix A:

$$g(U_{2k}, U_{2k}) \rightarrow g(U_{2k}, U_{2k}) - i\alpha_{y_k}, \qquad (13a)$$

$$g(U_{2k-1}, U_{2k-1}) \rightarrow g(U_{2k-1}, U_{2k-1}) - i\alpha_{x_k}. \qquad (13b)$$

As a result, all derivations in this paper can be done by first ignoring $\alpha_x$, then replacing the noninteracting Green's functions with these rules. For this reason and for readability, we will keep these replacements implicit in Wick matrices, but explicit otherwise.

Finally, Eq. (8) can be extended to the calculations of arbitrary Green's functions. The rule for doing so is as follows: whenever one introduces a product $-i\hat{c}(Y)\hat{c}^\dagger(Y')$ under the time-ordering operator in Eq. (5), one must add the corresponding Keldysh points in the Wick determinant of Eq. (8):

$$\begin{bmatrix} X, U_1, \ldots, U_{2n} \\ X', U_1, \ldots, U_{2n} \end{bmatrix} \rightarrow \begin{bmatrix} X, Y, U_1, \ldots, U_{2n} \\ X', Y', U_1, \ldots, U_{2n} \end{bmatrix}. \qquad (14)$$

If $Y$ and $Y'$ share the same time and orbital index $y$, we have the possibility to introduce terms of the form $-i[\hat{c}(Y)\hat{c}^\dagger(Y') + \alpha_y]$ in the definition of the Green's function. In that case, one must replace $g(Y, Y') \rightarrow g(Y, Y') - i\alpha_y$ in the diagonal of the Wick matrix. Again, to improve readability, we will keep this replacement implicit in Wick matrices, but explicit otherwise.

### B. A few properties of Wick determinants

Wick determinants have the general properties of determinants: exchanging two Keldysh points on either the first or the second line of the left-hand side of Eq. (10) leaves the Wick determinant unchanged up to a factor $(-1)$. An important property of the formalism, as already shown in Ref. [24], is that for $n > 0$:

$$\sum_{\{a_k\}} (-1)^{\sum_{k=1}^n a_k} \begin{bmatrix} U_1, \ldots, U_{2n} \\ U_1, \ldots, U_{2n} \end{bmatrix} = 0, \qquad (15)$$

for any times $u_1, \ldots, u_n$ and orbital indices $x_1, \ldots, x_n$ and $y_1, \ldots, y_n$. This relation expresses the fact that vacuum diagrams are automatically canceled by the sum over the Keldysh indices, even before any integration over time. It is proven in the usual way in the Keldysh formalism, by considering the largest $u_k$ time, say $k = p$. From the properties of the bare Green's functions, one can show that the elements of the Wick matrix, hence the determinant, are in fact all independent of $a_p$ (reflecting the fact that the largest time can be on the upper or the lower part of the contour). Therefore the sum over $a_p$ cancels the sum.

We will use the usual expansion of a determinant along one row or one column in terms of the cofactor matrix. It takes the form

$$\begin{bmatrix} A_1, \ldots, A_m \\ B_1, \ldots, B_m \end{bmatrix} = \sum_{k=1}^m (-1)^{k+1} g(A_k, B_1) \begin{bmatrix} A_1, \ldots \cancel{A_k} \ldots, A_m \\ \cancel{B_1}, B_2, \ldots, B_m \end{bmatrix} \qquad (16)$$

for the expansion along the first column and

$$\begin{bmatrix} A_1, \ldots, A_m \\ B_1, \ldots, B_m \end{bmatrix} = \sum_{k=1}^m (-1)^{k+1} g(A_1, B_k) \begin{bmatrix} \cancel{A_1}, \ldots \ldots, A_m \\ B_1, \cancel{B_k}, \ldots, B_m \end{bmatrix} \qquad (17)$$

for the expansion along the first row. The notation $\cancel{A_k}$ ($\cancel{B_k}$) stands for the fact that the corresponding row or column must be removed from the Wick matrix.

Last, we will also make a systematic use of the fact that the cofactor matrix is directly related to the inverse of the matrix,

$$(-1)^{i+j} \begin{bmatrix} A_1 \ldots \cancel{A_i}, \ldots \ldots, A_m \\ B_1, \ldots \cancel{B_j}, \ldots, B_m \end{bmatrix}$$
$$= \begin{bmatrix} A_1, \ldots, A_m \\ B_1, \ldots, B_m \end{bmatrix}^{-1}_{ji} \begin{bmatrix} A_1, \ldots, A_m \\ B_1, \ldots, B_m \end{bmatrix}. \qquad (18)$$

### C. Definition of the kernel $K$ for the one-body Green's function

In Ref. [24], a QMC scheme was defined directly on Eq. (8) so that a single QMC run could provide the value of $G^{aa'}_{xx'}(t, t')$ for a single pair of times $t$ and $t'$. In order to extend the technique and obtain a full curve (as a function of $t$) in a single run, a different form must be used. Performing the expansion of Eq. (17) on Eq. (8),

we obtain

$$G_{xx'}^{aa'}(t,t') = g_{xx'}^{aa'}(t,t') + \sum_{n \geqslant 1} \frac{i^n U^n}{n!} \int \prod_{k=1}^{n} du_k \sum_{\{x_k,y_k\}} \sum_{\{a_k\}} \left( \prod_{k=1}^{n} (-1)^{a_k} V_{x_k y_k}(u_k) \right)$$

$$\times \left( \sum_{p=1}^{2n} (-1)^p g[(x,t,a), U_p] \left[\!\!\left[ \begin{matrix} U_1, \ldots, U_{2n} \\ (x',t',a'), U_1, \ldots, \cancel{U_p}, \ldots, U_{2n} \end{matrix} \right]\!\!\right] + g[(x,t,a),(x',t',a')] \left[\!\!\left[ \begin{matrix} U_1, \ldots, U_{2n} \\ U_1, \ldots, U_{2n} \end{matrix} \right]\!\!\right] \right). \quad (19)$$

The last term of the sum vanishes for $n > 0$ due to Eq. (15). Factorizing the $g$ from the sum, we arrive at

$$G_{xx'}^{aa'}(t,t') = g_{xx'}^{aa'}(t,t') + \int du \sum_{b,y} (-1)^b g_{xy}^{ab}(t,u) K_{yx'}^{ba'}(u,t'), \quad (20)$$

where the kernel $K_{yx'}^{ba'}(u,t') = K(Y,X')$ with $Y = (y,u,b)$ is defined by

$$K(Y,X') \equiv (-1)^b \sum_{n \geqslant 1} \frac{i^n U^n}{n!} \int \prod_{k=1}^{n} du_k \sum_{\{x_k,y_k\}} \sum_{\{a_k\}} \left( \prod_{k=1}^{n} (-1)^{a_k} V_{x_k y_k}(u_k) \right) \sum_{p=1}^{2n} (-1)^p \delta_c(Y,U_p) \left[\!\!\left[ \begin{matrix} U_1, \ldots, U_{2n} \\ X', U_1, \ldots, \cancel{U_p}, \ldots, U_{2n} \end{matrix} \right]\!\!\right]. \quad (21)$$

Equations (20) and (21) will be the basis of one of the methods developed in this paper. Equation (21) will provide the means to get a full $t$ curve in a single calculation and Eq. (20) to relate the corresponding kernel to the Green's function $G$, the target of the calculation.

A symmetric kernel $\bar{K}$ may be derived following the exact same route but now expanding the Wick determinant along the first *column* using Eq. (16). We find

$$G_{xx'}^{aa'}(t,t') = g_{xx'}^{aa'}(t,t') + \int du \sum_{b,y} (-1)^b \bar{K}_{xy}^{ab}(t,u) g_{yx'}^{ba'}(u,t'), \quad (22)$$

where the kernel $\bar{K}$ is defined by

$$\bar{K}(X,Y) \equiv (-1)^b \sum_{n \geqslant 1} \frac{i^n U^n}{n!} \int \prod_{k=1}^{n} du_k \sum_{\{x_k,y_k\}} \sum_{\{a_k\}} \left( \prod_{k=1}^{n} (-1)^{a_k} V_{x_k y_k}(u_k) \right) \sum_{p=1}^{2n} (-1)^p \delta_c(Y,U_p) \left[\!\!\left[ \begin{matrix} X, U_1, \ldots, \cancel{U_p}, \ldots, U_{2n} \\ U_1, \ldots, U_{2n} \end{matrix} \right]\!\!\right]. \quad (23)$$

### D. Definition of the kernel $L$ of the $F$ Green's function

Let us define a new Green's function with four operators, the $F$ function. As we shall see, the $F$ Green's function can also be represented in terms of a kernel so that we will be able to design a direct QMC method to calculate it. Its interest stems from the fact that it can be used to reconstruct $G$ while the corresponding QMC technique will be more precise at high frequency. It is defined as

$$F_{xx'z}^{aa'}(t,t') \equiv (-i)^2 \langle T_c \hat{\mathbf{c}}(x,t,a) \hat{\mathbf{c}}^\dagger(x',t',a') [\hat{\mathbf{c}}^\dagger(z,t',a') \hat{\mathbf{c}}(z,t',a') - \alpha_z] \rangle. \quad (24)$$

In the next paragraph, we shall prove that $F$ is essentially equal to $\bar{K}$ (up to interacting matrix elements). The function $F$ is known to provide a better estimate of the Green's function. It has been used in the context of the numerical renormalization group (NRG) [47] as well as in imaginary time QMC methods as an *improved estimator* [48].

The expansion of $F$ reads

$$F_{xx'z}^{aa'}(t,t') = -\sum_{n \geqslant 0} \frac{i^n U^n}{n!} \int \prod_{k=1}^{n} du_k \sum_{\{x_k,y_k\}} \sum_{\{a_k\}} \left( \prod_{k=1}^{n} (-1)^{a_k} V_{x_k y_k}(u_k) \right) \left[\!\!\left[ \begin{matrix} (x,t,a), (z,t',a'), U_1, \ldots, U_{2n} \\ (x',t',a'), (z,t',a'), U_1, \ldots, U_{2n} \end{matrix} \right]\!\!\right]. \quad (25)$$

To obtain the kernel of $F$, we expand the determinant along its first row using Eq. (17),

$$F_{xx'z}^{aa'}(t,t') = -\sum_{n \geqslant 0} \frac{i^n U^n}{n!} \int \prod_{k=1}^{n} du_k \sum_{\{x_k,y_k\}} \sum_{\{a_k\}} \left( \prod_{k=1}^{n} (-1)^{a_k} V_{x_k y_k}(u_k) \right)$$

$$\times \left( \sum_{p=1}^{2n} (-1)^{p+1} g((x,t,a), U_p) \left[\!\!\left[ \begin{matrix} (z,t',a'), U_1, \ldots, U_{2n} \\ (x',t',a'), (z,t',a'), U_1, \ldots, \cancel{U_p}, \ldots, U_{2n} \end{matrix} \right]\!\!\right] \right.$$

$$\left. + g((x,t,a),(x',t',a')) \left[\!\!\left[ \begin{matrix} (z,t',a'), U_1, \ldots, U_{2n} \\ (z,t',a'), U_1, \ldots, U_{2n} \end{matrix} \right]\!\!\right] - g((x,t,a),(z,t',a')) \left[\!\!\left[ \begin{matrix} (z,t',a'), U_1, \ldots, U_{2n} \\ (x',t',a'), U_1, \ldots, U_{2n} \end{matrix} \right]\!\!\right] \right). \quad (26)$$

Identifying the two last terms with the corresponding expansion of $G$, we arrive at

$$F_{xx'z}^{aa'}(t, t') = -g_{xx'}^{aa'}(t, t')[G_{zz}^{<}(t', t') - i\alpha_z] + g_{xz}^{aa'}(t, t')G_{zx'}^{<}(t', t') - \int du \sum_{b,y} (-1)^b g_{xy}^{ab}(t, u)L_{yx'z}^{ba'}(u, t'), \quad (27)$$

where the kernel $L$ is defined by

$$L_{yx'z}^{ba'}(u, t') \equiv (-1)^b \sum_{n \geqslant 1} \frac{i^n U^n}{n!} \int \prod_{k=1}^{n} du_k \sum_{\{x_k, y_k\}} \sum_{\{a_k\}} \left( \prod_{k=1}^{n} (-1)^{a_k} V_{x_k y_k}(u_k) \right)$$

$$\times \sum_{p=1}^{2n} (-1)^{p+1} \delta_c((y, u, b), U_p) \left[\!\!\left[ \begin{matrix} (z, t', a'), U_1, \ldots, U_{2n} \\ (x', t', a'), (z, t', a'), U_1, \ldots, \cancel{U_p}, \ldots, U_{2n} \end{matrix} \right]\!\!\right]. \quad (28)$$

### E. Relation between $F$, $\bar{K}$, and $G$: Equations of motion

Here, we show that the expressions for the different kernels can be formally integrated to provide connections between the different kernels and Green's functions. We will arrive at expressions that are essentially what can be obtained directly using equations of motion.

We start with the expression of $\bar{K}$, Eq. (23). The first step is to realize that the sum over the $2n$ determinants provides identical contributions to the kernel. Indeed, odd $p = 2k - 1$ and even $p = 2k$ values of $p$ provide identical contributions due to the symmetry of $V_{xy}$. Similarly, odd values $p = 2k - 1$ have the same contribution as $p = 1$ as can be shown by using the symmetry properties of the determinant and exchanging the role of $U_1 \leftrightarrow U_{2k-1}$ and $U_2 \leftrightarrow U_{2k}$ in the sums and integration. We arrive at

$$\bar{K}_{xy}^{ab}(t, u) = (-1)^b \sum_{n \geqslant 1} \frac{i^n U^n}{n!} \int du_1 \sum_{x_1, y_1} \sum_{a_1} (-1)^{a_1} V_{x_1, y_1}(u_1) \int \prod_{k=2}^{n} du_k \sum_{\substack{\{x_k, y_k\} \\ k \geqslant 2}} \sum_{\substack{\{a_k\} \\ k \geqslant 2}} \left( \prod_{k=2}^{n} (-1)^{a_k} V_{x_k y_k}(u_k) \right)$$

$$\times 2n \, \delta_c(U_1, (y, u, b)) \left[\!\!\left[ \begin{matrix} (x, t, a), U_2, U_3, \ldots, U_{2n} \\ U_1, U_2, U_3, \ldots, U_{2n} \end{matrix} \right]\!\!\right]. \quad (29)$$

We can now perform explicitly the integral over $u_1$ where the delta function yields, for $u \in [0, t_M]$ ($\bar{K}$ is zero otherwise),

$$\bar{K}_{xy}^{ab}(t, u) = 2iU \sum_{n \geqslant 1} \frac{i^{n-1} U^{n-1}}{(n-1)!} \sum_{y_1} V_{y, y_1}(u) \int \prod_{k=2}^{n} du_k \sum_{\substack{\{x_k, y_k\} \\ \{a_k\} \\ k \geqslant 2}} \left( \prod_{k=2}^{n} (-1)^{a_k} V_{x_k y_k}(u_k) \right) \left[\!\!\left[ \begin{matrix} (x, t, a), (y_1, u, b), U_3, \ldots, U_{2n} \\ (y, u, b), (y_1, u, b), U_3, \ldots, U_{2n} \end{matrix} \right]\!\!\right], \quad (30)$$

$$\bar{K}_{xy}^{ab}(t, u) = 2iU \sum_{z} V_{y,z}(u) \sum_{n \geqslant 0} \frac{i^n U^n}{n!} \int \prod_{k=1}^{n} du_k \sum_{\substack{\{x_k, y_k\} \\ \{a_k\}}} \left( \prod_{k=1}^{n} (-1)^{a_k} V_{x_k y_k}(u_k) \right) \left[\!\!\left[ \begin{matrix} (x, t, a), (z, u, b), U_1, \ldots, U_{2n} \\ (y, u, b), (z, u, b), U_1, \ldots, U_{2n} \end{matrix} \right]\!\!\right], \quad (31)$$

$$\bar{K}_{xy}^{ab}(t, u) = -2iU \sum_z V_{yz}(u)F_{xyz}^{ab}(t, u). \quad (32)$$

This shows the kernel $\bar{K}$ is no more than a sum of two-particle Green's functions. The relation between $\bar{K}$ and $G$ in Eq. (22) can then be transformed into

$$G_{xx'}^{aa'}(t, t') = g_{xx'}^{aa'}(t, t') - 2iU \int du \sum_{b,y} (-1)^b$$

$$\times \sum_z V_{yz}(u)F_{xyz}^{ab}(t, u)g_{yx'}^{ba'}(u, t'), \quad (33)$$

which can be used to reconstruct $G$ from the knowledge of $F$. This relation is the well-known equation of motion for $G$. It also shows that $F$ is essentially the convolution of $G$ with the self-energy.

As a side note, we show in Appendix B that the kernel $L$ can also be expressed in terms of Green's functions by following the same formalism, in accordance with the equation of motion for $F$.

### F. Retarded and advanced kernels

As the retarded (or advanced) Green's functions directly give the spectral functions, they are of particular interest. At equilibrium, they contain all information which can be obtained from the Keldysh Green's function. We show here simple relations to compute them from the kernels $K$, $\bar{K}$, or $L$.

The retarded and advanced Green's functions relate to the lesser and greater Green's functions as follows:

$$G_{xx'}^{R}(t, t') = \theta(t - t')[G_{xx'}^{>}(t, t') - G_{xx'}^{<}(t, t')], \quad (34)$$

$$G_{xx'}^{A}(t, t') = \theta(t' - t)[G_{xx'}^{<}(t, t') - G_{xx'}^{>}(t, t')], \quad (35)$$

where $\theta$ is the Heaviside function. From the definitions of the time-ordered and time-antiordered Green's functions, these

can also be written as

$$G_{xx'}^R(t, t') = G_{xx'}^{a0}(t, t') - G_{xx'}^{a1}(t, t'), \quad (36)$$

$$G_{xx'}^A(t, t') = G_{xx'}^{0a}(t, t') - G_{xx'}^{1a}(t, t'), \quad (37)$$

where $a$ can be any Keldysh index. These are also valid for the noninteracting $g$. As $\bar{K}$ is a sum of Green's functions, one may define in the same way a retarded version of $\bar{K}$, denoted $\bar{K}^R$. We can see from Eq. (32) and the definition of $F$ in Eq. (24) that $\bar{K}^R$ follows the same properties:

$$\bar{K}_{xx'}^R(t, t') = \bar{K}_{xx'}^{a0}(t, t') - \bar{K}_{xx'}^{a1}(t, t'). \quad (38)$$

We now show a simple relation between $G^R$, $g^R$, and $\bar{K}^R$. Plugging Eq. (22) into Eq. (36), one gets

$$G_{xx'}^R(t, t') = g_{xx'}^R(t, t') + \int du \sum_y \left\{ \bar{K}_{xy}^{00}(t, u) \left[ g_{yx'}^{00}(u, t') \right. \right.$$
$$\left. - g_{yx'}^{01}(u, t') \right] - \bar{K}_{xy}^{01}(t, u) \left[ g_{yx'}^{10}(u, t') - g_{yx'}^{11}(u, t') \right] \right\}. \tag{39}$$

This simplifies into

$$G_{xx'}^R(t, t') = g_{xx'}^R(t, t') + \int du \sum_y \bar{K}_{xy}^R(t, u) g_{yx'}^R(u, t'). \quad (40)$$

Similar relations may be derived with $K$, $F$, and $L$. In fact, for any function from $K$, $F$, and $L$, which all depends on two times and two Keldysh indices, we choose to define a retarded and advanced function in the same way as Eqs. (34) and (35). As all of them are sums of Green's functions, one may show that they all verify similar properties as in Eqs. (36) and (37). Then from Eq. (20) follows

$$G_{xx'}^A(t, t') = g_{xx'}^A(t, t') + \int du \sum_y g_{xy}^A(t, u) K_{yx'}^A(u, t') \quad (41)$$

and from Eq. (27) follows

$$F_{xx'z}^A(t, t') = -g_{xx'}^A(t, t')[G_{zz}^<(t', t') - i\alpha_z] + g_{xz}^A(t, t')G_{zx'}^<(t', t)$$
$$- \int du \sum_y g_{xy}^A(t, u) L_{yx'z}^A(u, t'). \tag{42}$$

### III. QUANTUM MONTE CARLO TECHNIQUE

We now turn to the stochastic algorithms that will be used for the actual evaluations of the multidimensional integrals that define the expansion of the Green's function. These algorithms are direct extensions of the algorithm of Ref. [24] and inherit of most of its properties. The main interest lies in using kernels which permits the calculation of the full time dependency of the Green's function in a single QMC run.

#### A. Sampling of the kernel $K$

Let us first discuss the calculation of $G$ using the kernel $K$, using Eqs. (20) and (21). We rewrite by explicitly separating the sum over Keldysh indices (which will be summed explicitly) and the sum over space and integral over time (which will

be sampled using Monte Carlo). This separation was shown to be extremely important in Ref. [24]. The kernel takes the form

$$K(Y, X') = (-1)^b \sum_{n \geqslant 1} \int \prod_{k=1}^n du_k \sum_{\{x_k, y_k\}} \sum_{p=1}^{2n} \sum_{a_p} (-1)^{a_p}$$
$$\times \delta_c(Y, U_p) W_p^n(X', \{U_k\}, a_p), \tag{43}$$

$$W_p^n(X', \{U_k\}, a_p)$$
$$\equiv \frac{i^n U^n}{n!} \left( \prod_{k=1}^n V_{x_k y_k}(u_k) \right) \sum_{\substack{\{a_k\} \\ k \neq p}} \left( \prod_{k \neq p} (-1)^{a_k} \right) (-1)^p$$
$$\times \left[\!\!\left[ \begin{array}{c} U_1, \ldots, U_{2n} \\ (x', t', a'), U_1, \ldots, \not{U_p}, \ldots, U_{2n} \end{array} \right]\!\!\right]. \tag{44}$$

We define a configuration $\mathcal{C}$ as
  (i) the order $n$,
  (ii) a set of times $\{u_k \in [0, t_M]\}$ for $1 \leqslant k \leqslant n$,
  (iii) two sets of indices $\{x_k\}$ and $\{y_k\}$ for $1 \leqslant k \leqslant n$,
and the sum over all configurations as the integral over the $u_k$ and the sum over the $x_k, y_k$. For practical purpose, the time integrals run over a finite interval $[0, t_M]$. In accordance with the remark following Eq. (8), $t_M$ can be chosen to be any value larger than $t$ and $t'$ of the target Green's functions $G(t, t')$.

The kernel takes the form

$$K(Y, X') = (-1)^b$$
$$\times \sum_{\mathcal{C}} \left( \sum_{p=1}^{2n} \sum_{a_p} (-1)^{a_p} \delta_c(Y, U_p) W_p^n(X', \{U_k\}, a_p) \right), \tag{45}$$

where the sum over the configurations $\mathcal{C}$ is a compact notation for the sum and integrals of Eq. (43). We observe that a single configuration provides values of $K$ for $2n$ different points $Y$ through the delta function in the preceding expression. To sample the sum over configurations, we need to define a positive function $W(\mathcal{C})$ that will provide the (unnormalized) probability for the configuration $\mathcal{C}$ to be visited by the QMC algorithm. We define this weight as

$$W(\mathcal{C}) = \sum_{p=1}^{2n} \sum_{a=0,1} \left| W_p^n(X', \{U_k\}, a) \right|. \tag{46}$$

Noting $Z_{\text{QMC}} \equiv \sum_{\mathcal{C}} W(\mathcal{C})$, the kernel can be rewritten as

$$K(Y, X') = (-1)^b Z_{\text{QMC}} \left\langle \sum_{p=1}^{2n} \sum_{a_p} (-1)^{a_p} \right.$$
$$\left. \times \frac{W_p^n(X', \{U_k\}, a_p)}{W(\mathcal{C})} \delta_c((y, u, b), U_p) \right\rangle, \tag{47}$$

where the average is taken over the distribution $W(\mathcal{C})/Z_{\text{QMC}}$. $Z_{\text{QMC}}$ is an effective partition function associated to the QMC algorithm. Note that by construction, the weight $W(\mathcal{C})$ *controls* the measurement, i.e., $|W_p^n(X', \{U_k\}, a)| \leqslant W(\mathcal{C})$. This is an essential property for a reweighting technique since it guarantees that the weight $W_p^n(X', \{U_k\}, a)/W(\mathcal{C})$ does not

diverge (which can produce an infinite variance; for an example of this effect in the context of determinantal Monte Carlo see, e.g., Ref. [49]).

To sample $W(\mathcal{C})$ and evaluate $Z_{\mathrm{QMC}}$, we use the continuous time Monte Carlo technique that was discussed in detail in Ref. [24]. We use moves that change the order $n$ by $\pm 1$ so that all orders (up to a maximum one) can be calculated in a single run. The algorithm has very good ergodicity properties since the order $n = 0$ configuration is visited regularly. Each configuration $\mathcal{C}$ provides $2n$ values of $Y = (y, u, b)$ which are recorded by binning with the weight of Eq. (47).

The partial weights $W_p^n$ possess an essential *clusterization property*, which generalizes the one discovered in Ref. [24]: if one or several times $u_k$ goes to infinity (i.e., is far from $t'$), then all $W_p^n$ goes to 0. In other words the integrand is localized around $t'$. A detailed proof is provided in Appendix A. The point $X' = (x', t', a')$ is kept fixed during the calculation to *anchor* the integral around this point. An important consequence of the clusterization property is that the computational cost of the algorithm is uniform in $t_M$. Indeed, as one increases $t_M$, one simply adds regions of the configuration space that have a vanishingly small weight, hence do not contribute to the integral and do not get sampled.

Last, in order to calculate the factors $W_p^n$, we use the fact that they are made of the cofactors of the original matrix, hence can be rewritten as

$$
\begin{aligned}
&W_p^n(X', \{U_k\}, a_p) \\
&= -\frac{i^n U^n}{n!}\left(\prod_{k=1}^{n} V_{x_k y_k}(u_k)\right) \sum_{\substack{\{a_k\} \\ k \neq p}}\left(\prod_{k \neq p}(-1)^{a_k}\right) \\
&\quad \times \left\llbracket\begin{matrix} X, U_1, \ldots, U_{2n} \\ X', U_1, \ldots, U_{2n}\end{matrix}\right\rrbracket_{p1}^{-1} \left\llbracket\begin{matrix} X, U_1, \ldots, U_{2n} \\ X', U_1, \ldots, U_{2n}\end{matrix}\right\rrbracket.
\end{aligned}
\tag{48}
$$

This last form is very convenient since a single Wick matrix (and its inverse) needs to be stored and monitored during the calculation.

### B. Sampling of the kernel $L$

Following the same route for $L$ as was done for $K$, we can write

$$
\begin{aligned}
L_{yx'z}^{ba'}(u, t') = (-1)^b \sum_{n \geqslant 1} \int \prod_{k=1}^{n} du_k \sum_{\{x_k, y_k\}} \sum_{p=1}^{2n} \sum_{a_p}(-1)^{a_p} \\
\times \delta_c((y, u, b), U_p) W_{p+2}^n(X', \{U_k\}, a_p, z),
\end{aligned}
\tag{49}
$$

$$
\begin{aligned}
&W_{p+2}^n(X', \{U_k\}, a_p, z) \\
&\equiv \frac{i^n U^n}{n!}\left(\prod_{k=1}^{n} V_{x_k y_k}(u_k)\right) \sum_{\substack{\{a_k\} \\ k \neq p}}\left(\prod_{k \neq p}(-1)^{a_k}\right)(-1)^{p+1} \\
&\quad \times \left\llbracket\begin{matrix} (z, t', a'), U_1, \ldots, U_{2n} \\ (x', t', a'), (z, t', a'), U_1, \ldots, \cancel{U_p}, \ldots, U_{2n}\end{matrix}\right\rrbracket
\end{aligned}
\tag{50}
$$

thus defining $W_p^n$ for $p = 3, 4, \ldots, 2n + 2$. We also define $W_1^n$ and $W_2^n$ in the following way:

$$
\begin{aligned}
W_1^n(X', \{U_k\}, z) &\equiv -\frac{i^n U^n}{n!} \sum_{\{a_k\}}\left(\prod_{k=1}^{n}(-1)^{a_k} V_{x_k y_k}(u_k)\right) \\
&\quad \times \left\llbracket\begin{matrix} (z, t', a'), U_1, \ldots, U_{2n} \\ (z, t', a'), U_1, \ldots, U_{2n}\end{matrix}\right\rrbracket,
\end{aligned}
\tag{51}
$$

$$
\begin{aligned}
W_2^n(X', \{U_k\}, z) &\equiv \frac{i^n U^n}{n!} \sum_{\{a_k\}}\left(\prod_{k=1}^{n}(-1)^{a_k} V_{x_k y_k}(u_k)\right) \\
&\quad \times \left\llbracket\begin{matrix} (z, t', a'), U_1, \ldots, U_{2n} \\ (x', t', a'), U_1, \ldots, U_{2n}\end{matrix}\right\rrbracket.
\end{aligned}
\tag{52}
$$

These two extra values are necessary to compute $G_{zz}^<(t', t')$ and $G_{zx'}^<(t', t')$, which are needed to obtain $F$, as can be seen in Eq. (27). Moreover, they do not require extra computation time, as they are a direct by-product of the computation of the $W_p^n$ for $p > 2$. Indeed, in the same spirit as Eq. (48), the determinant within any $W_p^n$ (for $p = 1, \ldots, 2n + 2$) can be replaced by

$$
\begin{aligned}
&(-1)^{p+1} \left\llbracket\begin{matrix} X, (z, t', a'), U_1, \ldots, U_{2n} \\ X', (z, t', a'), U_1, \ldots, U_{2n}\end{matrix}\right\rrbracket_{p1}^{-1} \\
&\quad \times \left\llbracket\begin{matrix} X, (z, t', a'), U_1, \ldots, U_{2n} \\ X', (z, t', a'), U_1, \ldots, U_{2n}\end{matrix}\right\rrbracket.
\end{aligned}
\tag{53}
$$

Again, a single Wick matrix is needed to get contributions to all $W_p^n$ (given a set of Keldysh indices), which is very convenient.

Configurations are defined in the same way as in the previous section, and the weight of a configuration $\mathcal{C}$ is now

$$
\begin{aligned}
W(\mathcal{C}) = &\left|W_1^n(X', \{U_k\}, z)\right| + \left|W_2^n(X', \{U_k\}, z)\right| \\
&+ \sum_{p=1}^{2n} \sum_{a=0,1}\left|W_{p+2}^n(X', \{U_k\}, a, z)\right|.
\end{aligned}
\tag{54}
$$

We define again $Z_{\mathrm{QMC}} \equiv \sum_{\mathcal{C}} W(\mathcal{C})$ (which however has a different value than in the previous section). Finally, $L$ can be written as

$$
\begin{aligned}
L_{yx'z}^{ba'}(u, t') = (-1)^b Z_{\mathrm{QMC}} &\Bigg\langle \sum_{p=1}^{2n} \sum_{a_p}(-1)^{a_p} \frac{W_{p+2}^n(X', \{U_k\}, a_p, z)}{W(\mathcal{C})} \\
&\times \delta_c((y, u, b), U_p)\Bigg\rangle
\end{aligned}
\tag{55}
$$

and, from Eq. (8), we get that the values of $G_{zz}^<(t', t')$ and $G_{zx'}^<(t', t')$ (needed to compute $F$) are

$$
G_{zz}^<(t', t') = -Z_{\mathrm{QMC}}\left\langle\frac{W_1^n(X', \{U_k\}, z)}{W(\mathcal{C})}\right\rangle,
\tag{56}
$$

$$
G_{zx'}^<(t', t') = Z_{\mathrm{QMC}}\left\langle\frac{W_2^n(X', \{U_k\}, z)}{W(\mathcal{C})}\right\rangle.
\tag{57}
$$

The Monte Carlo algorithm used to evaluate these averages is the same as in the previous section, except for the weight $W(\mathcal{C})$.

### C. A discussion of the Werner et al. approach [16]

In this paragraph, we discuss the relation of this work with a preceding work [15,16] that also implements an expansion in powers of $U$ within the Keldysh formalism. Although both results are consistent, Ref. [16] has two important limitations which are not present in the method presented here. First, it suffers from a very large sign problem that increases drastically with time, while we do not experience a sign problem. Typical data shown in Ref. [16] correspond to a maximum time of $t_M \approx 5/\Gamma$ between the switching of the interaction and the measurement of the observable while we found that $t_M \approx 20/\Gamma$ is needed to enter the stationary result at order $n = 8$ as shown in Fig. 1. A direct consequence of this issue is that Ref. [16] cannot access the small bias regime where the Kondo effect is present: since the Kondo temperature $T_K$ is typically much smaller than $\Gamma$, long simulation times $t_M \gg 1/T_K$ are needed to capture the Kondo physics. Second, the technique of Ref. [16] suffered from a very large sign problem outside of the electron-hole symmetry point so that only this point could be studied.

An interesting aspect of Ref. [16] is that some results could be obtained in regimes where the "sign" of the Monte Carlo calculation was very small, $\sim 10^{-3}$ (see for instance Fig. 5 of Ref. [15]). Such a small sign is usually associated with very large error bars that prevent practical calculations from being performed. In the rest of this section, we make a simple technical remark that explains the origin of this behavior.

The main expansion formula used in the present work is Eq. (8) which provides the expansion for the Keldysh Green's function $G_{xx'}^{aa'}(t, t')$. A similar formula [24] provides the sum of vacuum diagrams, sometimes called the Keldysh "partition function" $Z$,

$$Z \equiv \sum_{n \geqslant 0} \frac{i^n U^n}{n!} \int \prod_{k=1}^{n} du_k \sum_{\{x_k, y_k\}} \left( \prod_{k=1}^{n} V_{x_k y_k}(u_k) \right)$$
$$\times \sum_{\{a_k\}} \prod_{k=1}^{n} (-1)^{a_k} \left[\!\!\left[ \begin{matrix} U_1, \dots, U_{2n} \\ U_1, \dots, U_{2n} \end{matrix} \right]\!\!\right]. \tag{58}$$

We have $Z = 1$ in the Keldysh formalism, reflecting the unitarity of quantum mechanics. We see that (15) indeed implies $Z = 1$, and that the cancellation of vacuum diagrams is due to the sum over Keldysh indices. The integrand is identically zero.

Let's note $Z(\{U_i\})$, the integrand of Eq. (58) (without the sum over Keldysh indices):

$$Z(\{U_i\}) \equiv \frac{i^n U^n}{n!} \left( \prod_{k=1}^{n} (-1)^{a_k} V_{x_k y_k}(u_k) \right) \left[\!\!\left[ \begin{matrix} U_1, \dots, U_{2n} \\ U_1, \dots, U_{2n} \end{matrix} \right]\!\!\right]. \tag{59}$$

Reference [15] Monte Carlo samples the absolute value of this integrand $|Z(\{U_i\})|$ (the authors actually used auxiliary Ising variables but that does not impact the present argument). We also note $G(X, X', \{U_i\})$, the integrand of Eq. (8), and $Z_{\text{QMC}}$, the integral of $|Z(\{U_i\})|$:

$$Z_{\text{QMC}} \equiv \sum_{n \geqslant 0} \int \prod_{k=1}^{n} du_k \sum_{\{x_k, y_k\}} \sum_{\{a_k\}} |Z(\{U_i\})|. \tag{60}$$
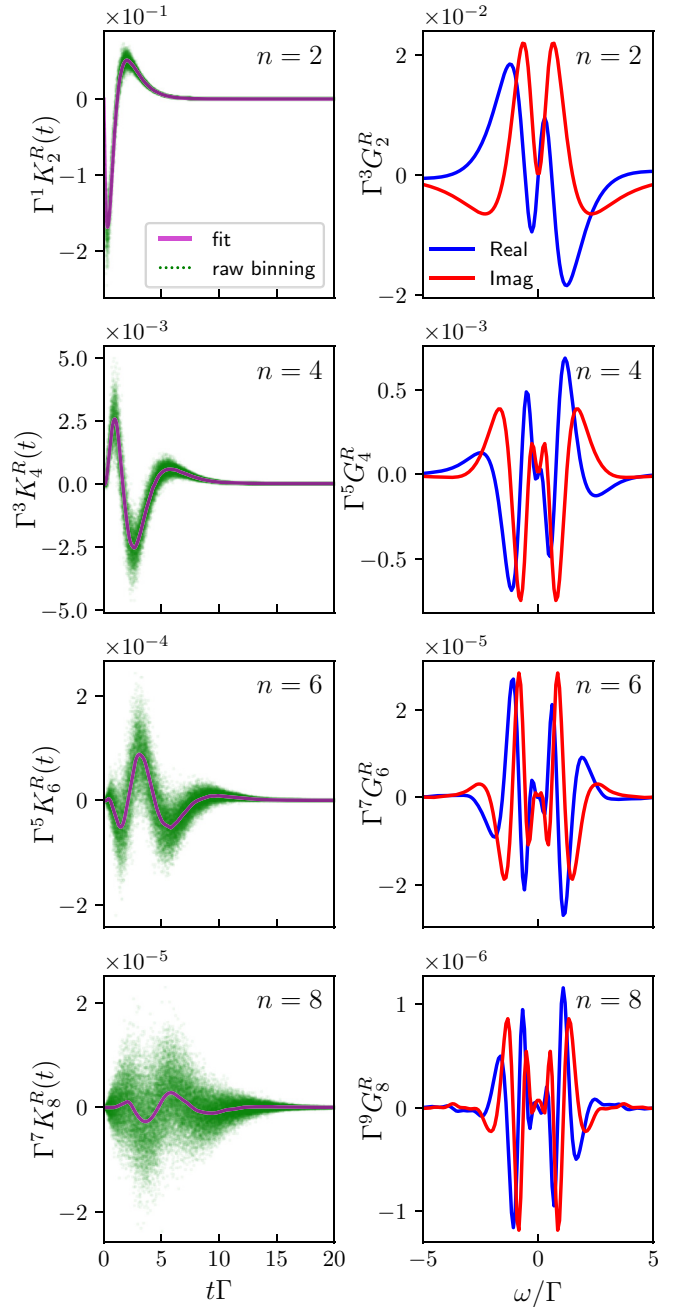


FIG. 1. First nonzero orders of the retarded kernel in time (left column), and corresponding retarded Green's function in frequency (right column), for the particle-hole symmetric model $\epsilon_d = 0$. The green dots in the left column correspond to the raw data of the binning with apparent noise arising from high frequencies. The purple lines are a fit of the kernel, shown for illustration purpose only, where the high-frequency noise has been subtracted by smearing the cumulative function of the kernel. Maximum time is $t_M = 20/\Gamma$. One can see (lower left panel) that at order $n = 8$ a lower integration time would not capture the whole kernel, thus the steady state would not be reached.

The weight of the QMC is $|Z(\{U_i\})|/Z_{\text{QMC}}$. We have

$$G_{xx'}^{aa'}(t, t') = \frac{\left\langle \frac{G(X, X', \{U_i\})}{|Z(\{U_i\})|} \right\rangle}{\left\langle \frac{Z(\{U_i\})}{|Z(\{U_i\})|} \right\rangle}, \tag{61}$$

where the average is the Monte Carlo average. The denominator of Eq. (61) is the QMC sign mentioned above. From $Z = 1$, we find that this QMC sign is simply given by $\langle Z(\{U_i\})/|Z(\{U_i\})|\rangle = 1/Z_{\text{QMC}}$.

Now, we note that the probability to visit order 0 is also $|Z(\varnothing)|/Z_{\text{QMC}} = 1/Z_{\text{QMC}}$. Therefore the average sign in the denominator of Eq. (61) is the probability to visit a configuration at zeroth order. This probability decreases when $U$ is increased, or at long time, when higher orders are sampled which explains why the QMC sign was observed to decrease drastically in Ref. [15]. However, this QMC sign is always positive and could *a priori* be computed very efficiently as an integral of a positive function using, e.g., the technique in Ref. [24]. A genuine sign problem can however result from the numerator of Eq. (61).

## IV. APPLICATION TO THE ANDERSON IMPURITY MODEL

We now turn to the illustration of our techniques with calculations done on the Anderson impurity model. The implementation of our technique was based on the TRIQS package [50]. We only present here results that showcase the technique and differ the exploration of the physics of the model, in particular the Kondo physics out of equilibrium, to the companion article of the present work [43]. We stress that the QMC technique is not restricted to impurity models and also applies to lattice models such as the Hubbard model.

### A. Definition of the model

In the Anderson impurity model, the impurity is described by the operators $\hat{\mathbf{d}}_\sigma^\dagger$ ($\hat{\mathbf{d}}_\sigma$) that create (destroy) an electron on the impurity with spin $\sigma$. The impurity is connected to two noninteracting electrodes via a tunneling Hamiltonian. Instead of providing explicitly this tunneling Hamiltonian and the Hamiltonian of the electrodes, it is simpler to write directly the noninteracting Green's function of the impurity. We work with its wide band form which is appropriate for the low-energy physics of a regular impurity model. The retarded Green's function reads in the frequency domain

$$g_{\sigma\sigma'}^R(\omega) = \frac{1}{\omega - \epsilon_d + i\Gamma}\delta_{\sigma\sigma'}, \qquad (62)$$

where the parameter $\Gamma$ sets the width of the resonance in the absence of electron-electron interactions and the on-site energy $\epsilon_d$ sets the resonance with respect to the Fermi level. Equation (62) fully defines the model at equilibrium. The model is made nontrivial through the interacting terms that read

$$\hat{H}_{\text{int}} = U\theta(t)\left(\hat{\mathbf{n}}_\uparrow - \tfrac{1}{2}\right)\left(\hat{\mathbf{n}}_\downarrow - \tfrac{1}{2}\right), \qquad (63)$$

where $\hat{\mathbf{n}}_\sigma = \hat{\mathbf{d}}_\sigma^\dagger \hat{\mathbf{d}}_\sigma$ is the impurity electronic density of spin $\sigma$ and the Heaviside function $\theta(t)$ represents the fact that the interaction is switched on at $t = 0$. The calculations are performed up to large times $t_M$ so that the system has relaxed to its stationary regime which corresponds to the interacting system at the bath temperature. All calculations are performed at very low temperature $k_B T = 10^{-4}\Gamma$, although the method is suitable for finite temperature as well.

The main output of our calculations is the expansion for the interacting retarded Green's function. Restricting ourselves to the stationary limit, it is a function of $t - t'$ only and can be studied in the frequency domain

$$G_{\sigma\sigma'}^R(t - t') = \delta_{\sigma\sigma'} \sum_{n=0}^{+\infty} G_n(t - t')U^n \qquad (64)$$

from which one can obtain the corresponding quantity in the frequency domain by fast Fourier transform,

$$G_{\sigma\sigma'}^R(\omega) = \delta_{\sigma\sigma'} \sum_{n=0}^{+\infty} G_n(\omega)U^n. \qquad (65)$$

Our technique typically provides the first $N = 10$ terms of this expansion as we show next. Last, we define the spectral function (or interacting local density of state)

$$A(\omega) = -\frac{1}{\pi}\text{Im}[G^R(\omega)] \qquad (66)$$

and the retarded self-energy $\Sigma^R(\omega)$,

$$G^R(\omega) = \frac{1}{\omega - \epsilon_d + i\Gamma - \Sigma^R(\omega)}. \qquad (67)$$

### B. Numerical results order by order

We now present the numerical data obtained by sampling the kernel $K$. The left panels of Fig. 1 show an example of the bare data for the retarded kernel $K^R(t)$ as they come out of the calculation for order $U^2$, $U^4$, $U^6$, and $U^8$ (top to bottom). Note that the noise in these data is mostly apparent; it corresponds to noise at very high frequency. This apparent noise reflects the fact that we have binned the curve $K^R(t)$ into a very fine grid (50 000 grid points in this calculation). An even finer grid would show even more apparent noise (since there would be even fewer Monte Carlo points per grid point). The corresponding cumulative function $\int_0^t K^R(u)du$ is however noiseless as can be seen from the example shown in Fig. 2 for $n = 8$.

The next step is to make a fast Fourier transform of $K_n^R(t)$ (not shown). The resulting $K_n^R(\omega)$ is relatively noisy at high frequency. Last, we obtain $G_n^R(\omega) = g^R(\omega)K_n^R(\omega)$ for $n \geqslant 1$ [from Eq. (41)] as shown in the right panel of Fig. 1. The factor $g^R(\omega)$, which decays at high frequency, very efficiently suppresses the high-frequency noise of the kernel data. The same noise-reduction mechanism has been reported in, e.g., Ref. [51] in the context of auxiliary-field Monte Carlo. We emphasize one aspect of these data which is rather remarkable: even though the eighth-order contribution $G_8^R(\omega)$ is the result of an eight-dimensional integral and is more than four orders of magnitude smaller than the second-order contribution $G_2^R(\omega)$, it can be obtained with high precision (the error bars are of the order of the thickness of the lines here). This is due to the recursive way these integrals are calculated as discussed in Ref. [24].

Using the definition Eq. (67) of the self-energy, we can obtain a recursive expression for $\Sigma_n^R$ in terms of the
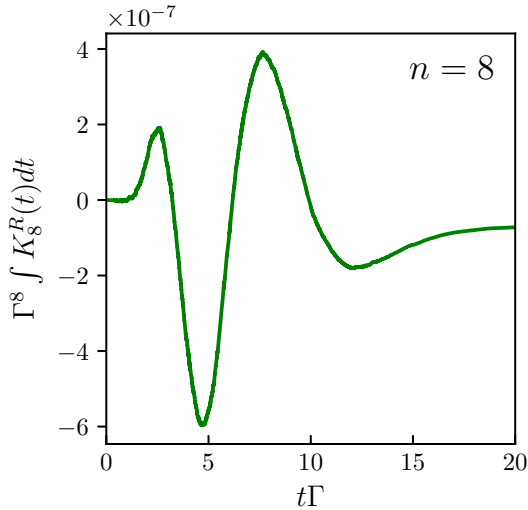
FIG. 2. Cumulative function $\int_0^t K_8^R(u)du$ obtained by integrating the raw data of the lower left panel of Fig. 1. Taking the integral gets rid of the apparent noise of the raw data whose origin is simply the presence of the binning grid in time.

Green's-function expansion:

$$\Sigma_n^R(\omega) = [g^R(\omega)]^{-2}G_n^R(\omega) - \sum_{k=1}^{n-1}\Sigma_k^R(\omega)G_{n-k}^R(\omega)g^R(\omega)^{-1}$$

$$(68)$$

for $n > 1$ with $\Sigma_1^R(\omega) = [g^R(\omega)]^{-2}G_1^R(\omega)$. The corresponding data are shown in Fig. 3 where we plot the coefficients $\Sigma_n^R(\omega)$ for $n = 2, 4, 6, 8$, and 10. The error bars increase with the order $n$ which we attribute to the fact that, since the self-energy only contains one-particle irreducible diagrams, it is the subject of many cancellations of terms. Indeed, one finds that the decay of $\Sigma_n^R(\omega)$ with $n$ is rather rapid with seven orders of magnitude between the first and the tenth order.

Our first benchmark uses a reference calculation made by Yamada [52]. The result at order 2 is compared with the result of Yamada in the left panel of Fig. 3 and found to be in excellent agreement. In his seminal work Yamada also provided analytical calculations at order 2 and 4 in the form of a low-frequency expansion for the particle-hole symmetric impurity,

$$\Sigma^R(U, \omega) = \Gamma \sum_{n,m} i^{m+1} s_{n,m}\left(\frac{\omega}{\Gamma}\right)^m\left(\frac{U}{\Gamma}\right)^n.$$

$$(69)$$

Table I shows the results of Yamada ($m = 1, 2$ and $n = 2, 4$) as well as ours (obtained by fitting our numerical data at low frequency). We find a good quantitative agreement with the Yamada results. Yamada also provided numerical results at $n = 4$ which are almost featureless and in very poor agreement with our data.

Our second method uses the kernel $L$ in order to calculate the Green's-function expansion. The bare data are very similar to the one obtained with the kernel $K$ method. By construction, the reconstruction of $G$ with $L$ involves $G_n(\omega) \sim g(\omega)^2 L_{n-1}(\omega)$ so that the high-frequency noise is expected to behave better with $L$ than with $K$ [the factor $g(\omega)^2$ effectively suppresses the high frequency]. Figure 4 shows a comparison of the errors obtained on $\Sigma_4^R(\omega)$ using the two methods. We find that the error using the $L$ method is essentially frequency independent while the error with the $K$ method depends strongly on frequency. In most cases the $L$ method is preferred but at small frequency, we have observed that the $K$ method can provide smaller error bars.

### C. Numerical results for the spectral function

Once the Green's function or self-energy has been obtained up to a certain order, the last task is to extract the physics information from this expansion. The most naive approach is to compute the truncated series up to a certain maximum order $N$,

$$\Sigma^R(U, \omega) \approx \sum_{n=1}^{N}\Sigma_n^R(\omega)U^n.$$

$$(70)$$

We find that the series has a convergence radius $U_c \approx 6\Gamma$ at the particle symmetry point $\epsilon_d = 0$ while this convergence radius decreases down to $U_c \approx 4\Gamma$ in the asymmetric case $\epsilon_d = \Gamma$. These convergence radii fix the maximum strength
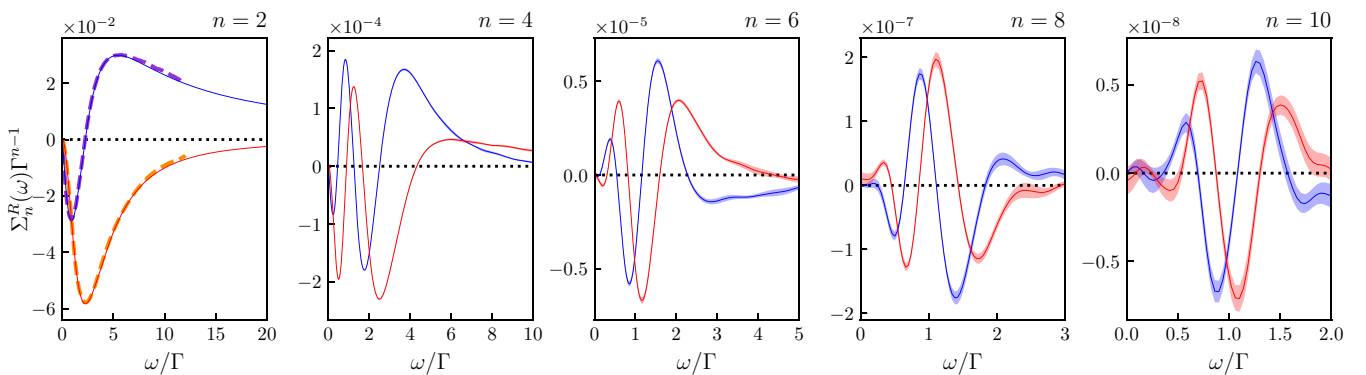


FIG. 3. First terms $\Sigma_n^R(\omega)$ of the development of the retarded self-energy in the particle-hole symmetric case ($\epsilon_d = 0$) for $n = 2, 4, 6, 8$, and 10 (plain lines, real part in blue and imaginary part in red). These curves are obtained in a single Monte Carlo run. Error bars are shown as shaded areas. A previous result at order 2 from Yamada [52] is shown in dashed lines. Note the decreasing scale with $n$. Maximum integration time is $t_M = 20/\Gamma$.

TABLE I. First coefficients $s_{n,m}$ (real) of the self-energy Taylor series $\Sigma(U,\omega)/\Gamma = \sum_{n,m} i^{m+1} s_{n,m} (U/\Gamma)^n (\omega/\Gamma)^m$ on the equilibrium symmetric model $\epsilon_d = 0$. Coefficients in powers of $\omega$ have been obtained by fitting the bare data by a polynomial. We find a good agreement with analytical calculations from Ref. [52] (second and fifth columns), as well as with Bethe ansatz exact calculations from Ref. [53] (third, sixth and eighth columns).

| $m$ | $n=2$ (QMC) | $n=2$ (Yamada) | $n=2$ (Bethe) | $n=4$ (QMC) | $n=4$ (Yamada) | $n=4$ (Bethe) | $n=6$ (QMC) | $n=6$ (Bethe) |
|---|---|---|---|---|---|---|---|---|
| 0 | $0 \pm 1 \times 10^{-5}$ | 0 | | $0 \pm 2 \times 10^{-6}$ | 0 | | $0 \pm 1 \times 10^{-7}$ | |
| 1 | $5.39(4) \times 10^{-2}$ | $5.3964 \times 10^{-2}$ | $5.3964 \times 10^{-2}$ | $5.7(0) \times 10^{-4}$ | $5.6771 \times 10^{-4}$ | $5.6482 \times 10^{-4}$ | $2.(1) \times 10^{-6}$ | $2.5119 \times 10^{-6}$ |
| 2 | $5.03(6) \times 10^{-2}$ | $5.0660 \times 10^{-2}$ | | $1.9(9) \times 10^{-3}$ | $2.0079 \times 10^{-3}$ | | $3.(1) \times 10^{-5}$ | |
| 3 | $3.67(5) \times 10^{-2}$ | | | $4.3(4) \times 10^{-3}$ | | | $1.(5) \times 10^{-4}$ | |
| 4 | $2.17(2) \times 10^{-2}$ | | | $6.2(4) \times 10^{-3}$ | | | $4.7(1) \times 10^{-4}$ | |

of $U$ that one can study using the naive truncated series approach.

The data for the self-energy (second and fourth panels) and corresponding spectral functions (first and third panels) are shown in Fig. 5 for the symmetric case (upper two panels, $\epsilon_d = 0$ and $U = 5\Gamma$) and asymmetric case (lower two panels, $\epsilon_d = \Gamma$ and $U = 3\Gamma$). For these values of interaction, the error in our calculation is dominated by the finite truncation of the series (negligible error due to the statistical Monte Carlo sampling) and is of the order of the linewidth. Figure 5 also shows the NRG results that we use to benchmark our calculations and that are in excellent agreement with our data. The NRG calculation is the same as in the companion paper [43], where it is described in details. Note that in order to obtain this agreement, the precision of the NRG calculations had to be pushed much further than what is typically done in the field indicating that the QMC method is very competitive, in particular at large frequencies.

Qualitatively, the strength of interaction that could be reached using the truncated series corresponds to the onset of

the Kondo effect: one observes in the upper panel of Fig. 5 that the Kondo peak starts to form around $\omega = 0$, its width is significantly narrower than without interaction and the premisses of the side peaks at $\pm U/2$ can be seen. In order to observe well established Kondo physics, one must therefore go beyond
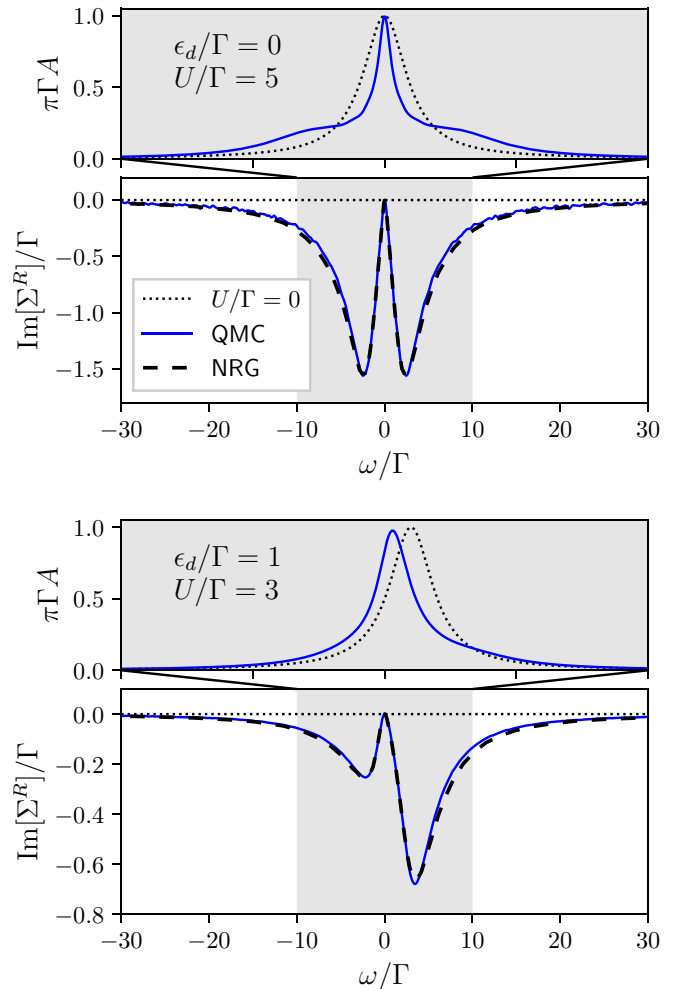


FIG. 5. Truncated series for the self-energy $\Sigma^R(\omega)$ at $\epsilon_d = 0$ and $U = 5\Gamma$ (second panel) and $\epsilon_d = \Gamma$ and $U = 3\Gamma$ (fourth panel) up to $N = 10$ orders in perturbation theory. The first and third panels show the corresponding spectral function. The Monte Carlo results (blue plain lines) are consistent with nonperturbative NRG calculations (dashed lines). The noninteracting situation is shown as dotted lines. Maximum integration time is $t_M = 20/\Gamma$.



FIG. 4. Statistical error of $\Sigma_4$ in the symmetric model at equilibrium, with increasing number of Monte Carlo steps. The $K$ kernel method (dotted lines) and the $L$ kernel method (plain line) are compared for different frequencies (different symbols). The error with the $L$ method is constant with frequencies, whereas the $K$ method accuracy worsens with increasing $\omega$. At large frequencies ($\omega > \Gamma$) the error is smaller when using the $L$ method.

the convergence radius wall. This is in fact rather natural; the convergence radius corresponds to poles or singularities in the complex $U$ plane which themselves correspond to the characteristic energy scales of the system. Getting past this "convergence radius wall" is crucial and is the subject of the companion paper to the present paper.

## V. CONCLUSION

In this paper, we have presented a quantum Monte Carlo algorithm that allows one to calculate the out-of-equilibrium Green's functions of an interacting system, order by order in powers of the interaction coupling constant $U$. We applied it to the Anderson model in the quantum dot geometry and obtained up to ten orders of the Green's function and self-energy. A detailed benchmark was also presented against NRG computations, after a simple summation of the series at weak coupling. Our results were obtained at almost zero temperature, but we found that the method works equally well at finite temperature or out of equilibrium. It works equally well for transient response to an interaction quench or at long time where a stationary regime has been reached.

The method presented here has the great advantage to produce the perturbative expansion *at infinite time*, i.e., directly in the steady state. Its complexity is uniform in time: it does not grow at long time, contrary to other QMC approaches. The drawback, like any "diagrammatic" QMC, is that we have just produced the perturbative series of, e.g., the Green's function and the self-energy. At weak coupling, we can simply sum it, as shown earlier in the benchmark. However, at intermediate coupling, simply summing the series with partial sums will fail. Most quantities have a finite radius $R$ of convergence in

$U$: for $U > R$, the series diverges. In Ref. [24], we showed how to use well-known conformal transformation resummation technique to solve this problem and obtain density of particle on the dot vs $U$ up to $U = \infty$. How to generalize this idea to make it work for real frequency Green's functions and also to control the amplification of stochastic noise due to such resummation will be addressed in a separate publication [43].

## APPENDIX A: PROOF OF THE CLUSTERIZATION PROPERTY OF THE KERNEL $K$

In this Appendix, we extend the proof of the clusterization property of Ref. [24] for the Kernel $K$, $\bar{K}$, and $L$. We want to show that, if some of the times $u_i$ are sent to infinity in the integral in Eqs. (8), (21), (23), and (28), the sum under the integral vanishes (while each determinant taken individually does not). We will not try to prove here the stronger property that the integrals do indeed converge but we observe it empirically in the numerical computations.

Let us restart from the clusterization proof of Ref. [24] for Eq. (8) and examine the sum over the Keldysh indices:

$$S \equiv \sum_{\{a_k\}} \prod_{k=1}^{n} (-1)^{a_k} \left[\!\!\left[ \begin{matrix} (x,t,a), U_1, \dots, U_{2n} \\ (x',t',a'), U_1, \dots, U_{2n} \end{matrix} \right]\!\!\right] = \sum_{\{a_k\}} \prod_{k=1}^{n} (-1)^{a_k} \begin{vmatrix} g(X,X') & g(X,U_1) & \dots & g(X,U_{2n}) \\ g(U_1,X') & g(U_1,U_1) & \dots & g(U_1,U_{2n}) \\ \vdots & \vdots & \ddots & \vdots \\ g(U_{2n},X') & g(U_{2n},U_1) & \dots & g(U_{2n},U_{2n}) \end{vmatrix}. \tag{A1}$$

If some $u_i$ are sent to infinity, we can relabel them $u_{p+1}, \dots, u_n$. Since $g$ vanishes at large time (due to the presence of the bath), the determinants in the sum become diagonal by block,

$$S \approx \sum_{\{a_k\}} \prod_{k=1}^{n} (-1)^{a_k} \begin{vmatrix} g(X,X') & g(X,U_1) & \dots & g(X,U_{2p}) & 0 & \dots & 0 \\ g(U_1,X') & g(U_1,U_1) & \dots & g(U_1,U_{2p}) & 0 & \dots & 0 \\ \vdots & \vdots & \ddots & \vdots & \vdots & \ddots & \vdots \\ g(U_{2p},X') & g(U_{2p},U_1) & \dots & g(U_{2p},U_{2p}) & 0 & \dots & 0 \\ 0 & 0 & \dots & 0 & g(U_{2p+1},U_{2p+1}) & \dots & g(U_{2p+1},U_{2n}) \\ \vdots & \vdots & \ddots & \vdots & \vdots & \ddots & \vdots \\ 0 & 0 & \dots & 0 & g(U_{2n},U_{2p+1}) & \dots & g(U_{2n},U_{2n}) \end{vmatrix}. \tag{A2}$$

The upper-left determinant does not depend on $a_{p+1}, \dots, a_n$, so we can apply Eq. (15) to the bottom-right determinant and the sum $S$ vanishes.

Let us now turn to the kernel $K$ defined in Eq. (21). The situation is slightly different. First, with a simple relabelling, we can restrict ourselves to the case $p = 1$ in Eq. (21). Let us first split the $U$ into two subsets:

$$S = \sum_{\{a_k\}} \prod_{k=1}^{n} (-1)^{a_k} \begin{vmatrix} g(U_1, X') & g(U_1, U_2) & \dots & g(U_1, U_{2p}) & g(U_1, U_{2p+1}) & \dots & g(U_1, U_{2n}) \\ \vdots & \vdots & \ddots & \vdots & \vdots & \ddots & \vdots \\ g(U_{2p}, X') & g(U_{2p}, U_2) & \dots & g(U_{2p}, U_{2p}) & g(U_{2p}, U_{2p+1}) & \dots & g(U_{2p}, U_{2n}) \\ g(U_{2p+1}, X') & g(U_{2p+1}, U_2) & \dots & g(U_{2p+1}, U_{2p}) & g(U_{2p+1}, U_{2p+1}) & \dots & g(U_{2p+1}, U_{2n}) \\ \vdots & \vdots & \ddots & \vdots & \vdots & \ddots & \vdots \\ g(U_{2n}, X') & g(U_{2n}, U_2) & \dots & g(U_{2n}, U_{2p}) & g(U_{2n}, U_{2p+1}) & \dots & g(U_{2n}, U_{2n}) \end{vmatrix}. \tag{A3}$$

Some $u_i$ go to infinity. We distinguish two cases:

(1) If $u_1$ does not go to infinity, we can relabel the indices so that $u_{p+1}, \dots, u_n$ go to infinity.

(2) If $u_1$ goes to infinity, we can relabel the indices so that $u_1, \dots, u_p$ go to infinity.

In both cases, the upper-right part of the matrix vanishes and we get a block-trigonal determinant,

$$S \approx \sum_{\{a_k\}} \prod_{k=1}^{n} (-1)^{a_k} \begin{vmatrix} g(U_1, X') & g(U_1, U_2) & \dots & g(U_1, U_{2p}) & 0 & \dots & 0 \\ \vdots & \vdots & \ddots & \vdots & \vdots & \ddots & \vdots \\ g(U_{2p}, X') & g(U_{2p}, U_2) & \dots & g(U_{2p}, U_{2p}) & 0 & \dots & 0 \\ g(U_{2p+1}, X') & g(U_{2p+1}, U_2) & \dots & g(U_{2p+1}, U_{2p}) & g(U_{2p+1}, U_{2p+1}) & \dots & g(U_{2p+1}, U_{2n}) \\ \vdots & \vdots & \ddots & \vdots & \vdots & \ddots & \vdots \\ g(U_{2n}, X') & g(U_{2n}, U_2) & \dots & g(U_{2n}, U_{2p}) & g(U_{2n}, U_{2p+1}) & \dots & g(U_{2n}, U_{2n}) \end{vmatrix}$$

$$= \left( \sum_{a_1, \dots, a_p} \prod_{k=1}^{p} (-1)^{a_k} \left[\!\!\left[ \begin{matrix} U_1, \dots, U_{2p} \\ X', U_2, \dots, U_{2p} \end{matrix} \right]\!\!\right] \right) \times \left( \sum_{a_{p+1}, \dots, a_n} \prod_{k=p+1}^{n} (-1)^{a_k} \left[\!\!\left[ \begin{matrix} U_{2p+1}, \dots, U_{2n} \\ U_{2p+1}, \dots, U_{2n} \end{matrix} \right]\!\!\right] \right),$$

since the first determinant does not depend on $a_{p+1}, \dots, a_n$. The second term cancels because of (15).

## APPENDIX B: EXPRESSION OF THE KERNEL $L$ AS A SUM OF GREEN'S FUNCTIONS

We show here that the kernel $L$ can be expressed in terms of Green's functions. Starting from its definition Eq. (28), we follow the same steps as in Sec. II E. We first use the fact (due to determinant symmetry) that all terms of the sum over $p$ have the same contribution:

$$L_{yx'z}^{ba'}(u, t') = (-1)^b \sum_{n \geq 1} \frac{i^n U^n}{n!} \int \prod_{k=1}^{n} du_k \sum_{\{x_k, y_k\}} \sum_{\{a_k\}} \left( \prod_{k=1}^{n} (-1)^{a_k} V_{x_k y_k}(u_k) \right)$$

$$\times 2n\, \delta_c((y, u, b), U_1) \left[\!\!\left[ \begin{matrix} (z, t', a'), U_1, U_2, \dots, U_{2n} \\ (x', t', a'), (z, t', a'), U_2, \dots, U_{2n} \end{matrix} \right]\!\!\right]. \tag{B1}$$

Then we sum out the Dirac delta:

$$L_{yx'z}^{ba'}(u, t') = 2iU \sum_{z'} V_{yz'}(u) \sum_{n \geq 0} \frac{i^n U^n}{n!} \int \prod_{k=1}^{n} du_k \sum_{\{x_k, y_k\}} \sum_{\{a_k\}} \left( \prod_{k=1}^{n} (-1)^{a_k} V_{x_k y_k}(u_k) \right)$$

$$\times \left[\!\!\left[ \begin{matrix} (z, t', a'), (y, u, b), (z', u, b), U_1, \dots, U_{2n} \\ (x', t', a'), (z, t', a'), (z', u, b), U_1, \dots, U_{2n} \end{matrix} \right]\!\!\right]. \tag{B2}$$

The pattern of a three-particle Green's function can be recognized:

$$L_{yx'z}^{ba'}(u, t') = 2iU \sum_{z'} V_{yz'}(u) E_{yx'zz'}^{ba'}(u, t'), \tag{B3}$$

where $E$ is defined as

$$E_{yx'zz'}^{ba'}(u, t') \equiv (-i)^3 \langle T_c \hat{\mathbf{c}}(y, u, b) \hat{\mathbf{c}}^\dagger(x', t', a') [\hat{\mathbf{c}}^\dagger(z, t', a') \hat{\mathbf{c}}(z, t', a') - \alpha_z] [\hat{\mathbf{c}}^\dagger(z', u, b) \hat{\mathbf{c}}(z', u, b) - \alpha_{z'}] \rangle. \tag{B4}$$

[1] M. Först, C. Manzoni, S. Kaiser, Y. Tomioka, Y. Tokura, R. Merlin, and A. Cavalleri, Nat. Phys. **7**, 854 (2011).

[2] D. Fausti, R. I. Tobey, N. Dean, S. Kaiser, A. Dienst, M. C. Hoffmann, S. Pyon, T. Takayama, H. Takagi, and A. Cavalleri, Science **331**, 189 (2011).

[3] D. Nicoletti, E. Casandruc, Y. Laplace, V. Khanna, C. R. Hunt, S. Kaiser, S. S. Dhesi, G. D. Gu, J. P. Hill, and A. Cavalleri, Phys. Rev. B **90**, 100503(R) (2014).

[4] E. Casandruc, D. Nicoletti, S. Rajasekaran, Y. Laplace, V. Khanna, G. D. Gu, J. P. Hill, and A. Cavalleri, Phys. Rev. B **91**, 174502 (2015).

[5] D. Nicoletti and A. Cavalleri, Adv. Opt. Photon. **8**, 401 (2016).

[6] D. Nicoletti, D. Fu, O. Mehio, S. Moore, A. S. Disa, G. D. Gu, and A. Cavalleri, Phys. Rev. Lett. **121**, 267003 (2018).

[7] F. Nakamura, M. Sakaki, Y. Yamanaka, S. Tamaru, T. Suzuki, and Y. Maeno, Sci. Rep. **3**, 2536 (2013).

[8] A. Georges, G. Kotliar, W. Krauth, and M. J. Rozenberg, Rev. Mod. Phys. **68**, 13 (1996).

[9] G. Kotliar, S. Y. Savrasov, K. Haule, V. S. Oudovenko, O. Parcollet, and C. A. Marianetti, Rev. Mod. Phys. **78**, 865 (2006).

[10] H. Aoki, N. Tsuji, M. Eckstein, M. Kollar, T. Oka, and P. Werner, Rev. Mod. Phys. **86**, 779 (2014).

[11] S. R. White, Phys. Rev. Lett. **69**, 2863 (1992).

[12] S. R. White, Phys. Rev. B **48**, 10345 (1993).

[13] U. Schollwöck, Rev. Mod. Phys. **77**, 259 (2005).

[14] L. Mühlbacher and E. Rabani, Phys. Rev. Lett. **100**, 176403 (2008).

[15] P. Werner, T. Oka, and A. J. Millis, Phys. Rev. B **79**, 035320 (2009).

[16] P. Werner, T. Oka, M. Eckstein, and A. J. Millis, Phys. Rev. B **81**, 035108 (2010).

[17] M. Schiró and M. Fabrizio, Phys. Rev. B **79**, 153302 (2009).

[18] M. Schiró, Phys. Rev. B **81**, 085126 (2010).

[19] G. Cohen, D. R. Reichman, A. J. Millis, and E. Gull, Phys. Rev. B **89**, 115139 (2014).

[20] G. Cohen, E. Gull, D. R. Reichman, and A. J. Millis, Phys. Rev. Lett. **112**, 146802 (2014).

[21] G. Cohen, E. Gull, D. R. Reichman, and A. J. Millis, Phys. Rev. Lett. **115**, 266802 (2015).

[22] H.-T. Chen, G. Cohen, and D. R. Reichman, J. Chem. Phys. **146**, 054105 (2017).

[23] H.-T. Chen, G. Cohen, and D. R. Reichman, J. Chem. Phys. **146**, 054106 (2017).

[24] R. E. V. Profumo, C. Groth, L. Messio, O. Parcollet, and X. Waintal, Phys. Rev. B **91**, 245154 (2015).

[25] N. V. Prokof'ev and B. V. Svistunov, Phys. Rev. Lett. **81**, 2514 (1998).

[26] A. S. Mishchenko, N. V. Prokof'ev, A. Sakamoto, and B. V. Svistunov, Phys. Rev. B **62**, 6317 (2000).

[27] K. Van Houcke, E. Kozik, N. Prokof'ev, and B. Svistunov, Physics Procedia **6**, 95 (2010).

[28] N. Prokof'ev and B. Svistunov, Phys. Rev. Lett. **99**, 250201 (2007).

[29] N. V. Prokof'ev and B. V. Svistunov, Phys. Rev. B **77**, 125101 (2008).

[30] E. Gull, D. R. Reichman, and A. J. Millis, Phys. Rev. B **82**, 075109 (2010).

[31] E. Kozik, K. V. Houcke, E. Gull, L. Pollet, N. Prokof'ev, B. Svistunov, and M. Troyer, Europhys. Lett. **90**, 10004 (2010).

[32] L. Pollet, Rep. Prog. Phys. **75**, 094501 (2012).

[33] K. Van Houcke, F. Werner, E. Kozik, N. Prokof'ev, B. Svistunov, M. J. H. Ku, A. T. Sommer, L. W. Cheuk, A. Schirotzek, and M. W. Zwierlein, Nat. Phys. **8**, 366 (2012).

[34] S. A. Kulagin, N. Prokof'ev, O. A. Starykh, B. Svistunov, and C. N. Varney, Phys. Rev. Lett. **110**, 070601 (2013).

[35] S. A. Kulagin, N. Prokof'ev, O. A. Starykh, B. Svistunov, and C. N. Varney, Phys. Rev. B **87**, 024407 (2013).

[36] J. Gukelberger, E. Kozik, L. Pollet, N. Prokof'ev, M. Sigrist, B. Svistunov, and M. Troyer, Phys. Rev. Lett. **113**, 195301 (2014).

[37] Y. Deng, E. Kozik, N. V. Prokof'ev, and B. V. Svistunov, Europhys. Lett. **110**, 57001 (2015).

[38] Y. Huang, K. Chen, Y. Deng, N. Prokof'ev, and B. Svistunov, Phys. Rev. Lett. **116**, 177203 (2016).

[39] R. Rossi, T. Ohgoe, E. Kozik, N. Prokof'ev, B. Svistunov, K. Van Houcke, and F. Werner, Phys. Rev. Lett. **121**, 130406 (2018).

[40] K. Van Houcke, F. Werner, T. Ohgoe, N. V. Prokof'ev, and B. V. Svistunov, Phys. Rev. B **99**, 035140 (2019).

[41] R. Rossi, Phys. Rev. Lett. **119**, 045701 (2017).

[42] A. Moutenet, W. Wu, and M. Ferrero, Phys. Rev. B **97**, 085117 (2018).

[43] C. Bertrand, S. Florens, O. Parcollet, and X. Waintal, arXiv:1903.11646 [Phys. Rev. X (to be published)].

[44] A. N. Rubtsov and A. I. Lichtenstein, J. Exp. Theor. Phys. Lett. **80**, 61 (2004).

[45] W. Wu, M. Ferrero, A. Georges, and E. Kozik, Phys. Rev. B **96**, 041105(R) (2017).

[46] B. Gaury, J. Weston, M. Santin, M. Houzet, C. Groth, and X. Waintal, Phys. Rep. **534**, 1 (2014).

[47] R. Bulla, A. C. Hewson, and T. Pruschke, J. Phys.: Condens. Matter **10**, 8365 (1998).

[48] H. Hafermann, K. R. Patton, and P. Werner, Phys. Rev. B **85**, 205106 (2012).

[49] H. Shi and S. Zhang, Phys. Rev. E **93**, 033303 (2016).

[50] O. Parcollet, M. Ferrero, T. Ayral, H. Hafermann, I. Krivenko, L. Messio, and P. Seth, Comput. Phys. Commun. **196**, 398 (2015).

[51] E. Gull, P. Werner, O. Parcollet, and M. Troyer, Europhys. Lett. **82**, 57003 (2008).

[52] K. Yamada, Prog. Theor. Phys. **53**, 970 (1975).

[53] B. Horvatić and V. Zlatić, J. Phys. France **46**, 1459 (1985).